PAPER

Phononic thermal conductivity in silicene: the role of vacancy defects and boundary scattering

IOP Publishing Journal of Physics: Condensed Matter
J. Phys.: Condens. Matter **30** (2018) 155307 (9pp) https://doi.org/10.1088/1361-648X/aab422

Phononic thermal conductivity in silicene: the role of vacancy defects and boundary scattering

M Barati[1], T Vazifehshenas[1], T Salavati-fard[2] and M Farmanbar[3]

[1] Department of Physics, Shahid Beheshti University, G. C., Evin, Tehran 1983969411, Iran
[2] Department of Physics and Astronomy, University of Delaware, Newark, DE 19716, United States of America
[3] Computational Materials Science, MESA+ Institute for Nanotechnology, University of Twente, P.O. Box 217, 7500AE, Enschede, The Netherlands

E-mail: t-vazifeh@sbu.ac.ir

Received 7 January 2018, revised 1 March 2018
Accepted for publication 5 March 2018
Published 22 March 2018

Abstract

We calculate the thermal conductivity of free-standing silicene using the phonon Boltzmann transport equation within the relaxation time approximation. In this calculation, we investigate the effects of sample size and different scattering mechanisms such as phonon–phonon, phonon-boundary, phonon-isotope and phonon-vacancy defect. We obtain some similar results to earlier works using a different model and provide a more detailed analysis of the phonon conduction behavior and various mode contributions. We show that the dominant contribution to the thermal conductivity of silicene, which originates from the in-plane acoustic branches, is about 70% at room temperature and this contribution becomes larger by considering vacancy defects. Our results indicate that while the thermal conductivity of silicene is significantly suppressed by the vacancy defects, the effect of isotopes on the phononic transport is small. Our calculations demonstrate that by removing only one of every 400 silicon atoms, a substantial reduction of about 58% in thermal conductivity is achieved. Furthermore, we find that the phonon-boundary scattering is important in defectless and small-size silicene samples, especially at low temperatures.

Keywords: thermal conductivity, silicene, phonon, Boltzmann transport equation, vacancy defects, boundary scattering

(Some figures may appear in colour only in the online journal)

1. Introduction

Interest in two-dimensional (2D) materials and layered structures has been considerably growing during the last two decades, because of a wide variety of applications in nanotechnology. The discovery of graphene [1], a planar honeycomb structure of carbon atoms, was a milestone in the development of nano sciences due to its extraordinary properties such as high carrier mobility [1–5], room-temperature ballistic carrier transport [1, 3], high lattice stability [1, 2] and high mechanical strength [1].

Silicene, the 2D graphene-like structure of silicon, is slightly buckled (figure 1) in its most stable form. The buckling leads to some new characteristics [6, 7] which make silicene a promising alternative to graphene in the rapidly developing fields of thermoelectrics and nanoelectronics [8–10]. While the electronic properties of silicene have been extensively studied [11–13], its thermal transport features are still open for more investigations [14]. Graphene exhibits a high lattice thermal conductivity [15–18] which may be useful in some applications such as electronic cooling and heat spreading [19, 20]. Nevertheless, high lattice thermal conductivity is not appealing in thermoelectric devices where a very low thermal conductivity is required. Unlike graphene, silicene with a small lattice thermal conductivity [14] can be effectively used in thermoelectricity in future. Because of difficulties in

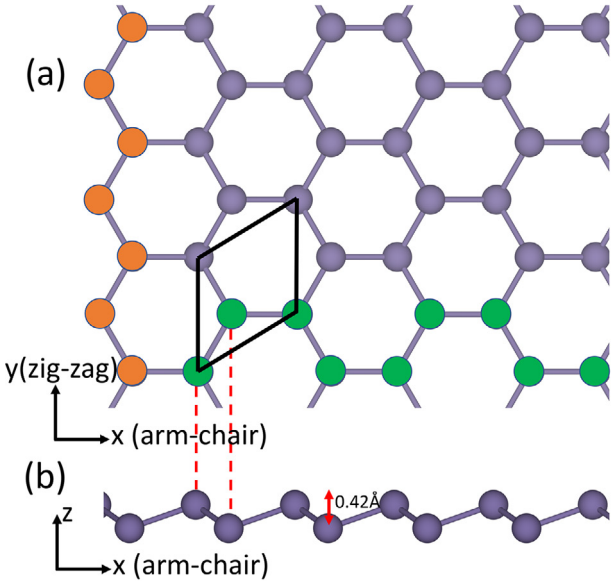

Figure 1. (a) Top and (b) side views of silicene. The unit cell is shown in black lines.

synthesizing free-standing silicene, the thermal conductivity of silicene has not been experimentally measured yet, but it has been calculated using a couple of numerical methods. Molecular dynamics (MD) simulations, which rigorously rely on the empirical interatomic potentials, predicted values of thermal conductivity in the range of 5 to 69 W mK^{-1} [21–25]. On the other hand, the predicted values of thermal conductivity of silicene from first-principles based calculations span 10–30 W mK^{-1} [14, 26–28]. In this approach, the harmonic second-order and anharmonic third-order interatomic force constants [29–37] are determined from first-principles using density functional perturbation theory as input parameters and then the phonon Boltzmann transport equation (PBTE) is solved. PBTE is a successful microscopic description for the intrinsic thermal conductivity of semiconductors and insulators which was first formulated by Peierls [38]. In PBTE, the variation of the phonon distribution with the temperature gradient is balanced by its changes due to the scattering processes. Instead of solving the PBTE self-consistently, which is computationally very expensive, it is common to employ the relaxation time approximation (RTA) in which the phonon lifetime is approximated as the sum over all the contributions from different scattering mechanisms [39, 40]. Comparing the results of full iterative calculations of intrinsic lattice thermal conductivity of silicene [8, 27] with those obtained from the RTA [14], shows that the RTA works well for the case of silicene. A recent review on this topic can be found in first chapter of 'Silicene' by Spencer and Morishita [41].

In this study, we use a theoretical approach to calculate the lattice thermal conductivity of free-standing monolayer silicene based on a numerical solution of the PBTE within RTA. We use the second- and third-order force constants obtained from the density functional theory (DFT) [27] to calculate the phononic thermal conductivity under different scattering mechanisms including the phonon–phonon, phonon-boundary, phonon-isotope and phonon-vacancy scatterings and study the effects of temperature and size of the system. Also, we investigate how various phonon modes contribute to the thermal conductivity and show that the in-plane acoustic modes carry most of the heat, in contrast to the case of graphene. Furthermore, we find that, among different elastic scattering mechanisms, the phonon-vacancy scattering has the most significant influence on the silicene thermal conductivity. This prediction for the vacancy effect is in good agreement with that of the MD simulation [25]. Our findings shed some light on how the figure of merit and thermoelectricity in silicene can be controlled.

The rest of the paper is organized as follows: in section 2, the theory is given and the method is explained in detail. The results are presented and discussed thoroughly in section 3. Finally, the highlights of this work are summarized in section 4.

2. Theory and method

We consider a free-standing monolayer silicene and calculate the thermal conductivity based on the linearized PBTE within the RTA. As we mentioned earlier, the PBTE can be solved using an iterative method too, however, it has been shown that the difference between calculated thermal conductivity of silicene by employing any of the two methods is small [14].

The contribution of all phonon modes to the thermal conductivity, κ, can be expressed as [42, 43]:

$$\kappa = \frac{\hbar^2}{Vk_BT^2}\sum_{\lambda}\omega_\lambda^2 v_\lambda^2 n_\lambda^0(1+n_\lambda^0)\tau_\lambda, \tag{1}$$

where $\hbar$, k_B, v_λ, n_λ^0 and τ_λ are the Planck constant over 2π, Boltzmann constant, phonon velocity of mode λ ($\lambda = (\mathbf{q}, s)$, where $\mathbf{q}$ stands for phonon wave vector and s denotes branch index), equilibrium distribution function and scattering time, respectively. Also, V and T are the volume of the unit cell and temperature. The phonon frequency of mode λ, ω_λ, is obtained from the dynamical matrix of the system, which its $(\alpha\beta)$ Cartesian component, $D^{\alpha\beta}(\mathbf{q})$, is given by [27]:

$$D_{jj'}^{\alpha\beta}(\mathbf{q}) = \frac{1}{\sqrt{M_jM_{j'}}}\sum_{\mathbf{R}'}\phi_{\mathbf{0}j\mathbf{R}'j'}^{\alpha\beta}e^{i\mathbf{q}.\mathbf{R}'}. \tag{2}$$

Here, $\phi_{\mathbf{0}j\mathbf{R}'j'}^{\alpha\beta}$ is the harmonic (second-order) force constant (corresponding to the displacement of atom $\mathbf{R} = 0, j$ in the α direction and the displacement of atom $\mathbf{R}', j'$ in the β direction) which can be extracted from the first-principles calculations, $\mathbf{R}'$ is the lattice vector of unit cell and M_j is the mass of jth atom in this unit cell. Since there is only one type of atom in silicene, so we set $M_{j/j'} = M$. The dispersion relations of different branches of phonons can be obtained from the zeros of the determinant of the dynamical matrix. We calculate phonon dispersions by diagonalization of the dynamical matrix which is obtained using the harmonic force constants taken from [27]. Figure 2 shows the phonon dispersion of free-standing silicene along some high symmetry directions. There are three acoustic branches (flexural acoustic (ZA), longitudinal acoustic (LA) and transverse acoustic (TA)) and three optical modes (flexural

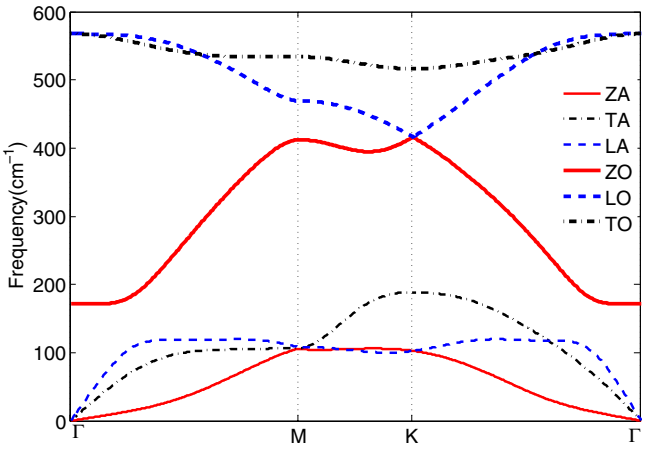

Figure 2. Phonon dispersion of monolayer silicene.

optical (ZO), longitudinal optical (LO) and transverse optical (TO)) as a result of two atoms per unit cell of silicene. In contrast to graphene, due to buckled structure of silicene, the flexural modes of silicene are not completely out-of-plane and can get coupled to the in-plane modes. As a result of this coupling, the selection rules for the phonon–phonon scattering in silicene is different from graphene [26, 27].

It is well known that the scattering processes play an important role in determining the thermal conductivity. Phonon–phonon, phonon-boundary, phonon-isotope and phonon-vacancy scatterings are the main mechanisms for the phonon transport [44]. Within the RTA, the scattering lifetime, τ_λ, can be calculated by employing the Matthiessen's rule as [39, 40]:

$$\frac{1}{\tau_\lambda} = \sum_i \frac{1}{\tau_\lambda^i}, \tag{3}$$

where τ_λ^i denotes the relaxation time of each scattering mechanism and the sum goes over all the possible mechanisms.

In a perfect lattice without any defects or rough boundaries, thermal conductivity is limited by the phonon–phonon scattering through the absorption and emission processes in which the following energy and quasi-momentum conservation laws are satisfied [29, 45]:

$$\omega_\lambda \pm \omega_{\lambda'} = \omega_{\lambda''} \tag{4}$$

$$\mathbf{q} \pm \mathbf{q}' = \mathbf{q}'' + \mathbf{G}. \tag{5}$$

Here, $\mathbf{G}$ is a reciprocal lattice vector. The relaxation time of the phonon–phonon scattering, $\tau_\lambda^{\mathrm{Ph}}$, can be expressed as [35, 46]

$$\tau_\lambda^{\mathrm{Ph}} = \frac{n_\lambda^0(1+n_\lambda^0)}{\sum_{\lambda'\lambda''}[W^+_{\lambda\lambda'\lambda''} + \frac{1}{2}W^-_{\lambda\lambda'\lambda''}]}, \tag{6}$$

where $W^\pm_{\lambda\lambda'\lambda''}$ is the phonon–phonon scattering rate for the absorption and emission processes [29, 35, 45, 46]

$$W^\pm_{\lambda\lambda'\lambda''} = \frac{\pi\hbar}{4N_0}\frac{(1+n_\lambda^0)(n_{\lambda'}^0 + \frac{1}{2} \pm \frac{1}{2})n_{\lambda''}^0}{\omega_\lambda\omega_{\lambda'}\omega_{\lambda''}} \times \left|V^\pm_{\lambda\lambda'\lambda''}\right|^2 \delta(\omega_\lambda \pm \omega_{\lambda'} - \omega_{\lambda''}). \tag{7}$$

In the above expression N_0 is the number of unit cells and the three-phonon scattering matrix elements of the phonon–phonon interaction, $V^\pm_{\lambda\lambda'\lambda''}$, are given by: [29, 45, 46]

$$V^\pm_{\lambda\lambda'\lambda''} = \sum_j \sum_{R'j'} \sum_{R''j''} \sum_{\alpha\beta\gamma} \phi^{\alpha\beta\gamma}_{0j,R'j',R''j''} \times \frac{e^\alpha_\lambda(j) e^\beta_{\pm\lambda'}(j') e^\gamma_{\lambda''}(j'')}{\sqrt{M_j M_{j'} M_{j''}}} \mathrm{e}^{\mathrm{i}(\pm\mathbf{q}').\mathbf{R}'} \mathrm{e}^{\mathrm{i}\mathbf{q}''.\mathbf{R}''}, \tag{8}$$

which depend on the third-order interatomic force constants, $\phi^{\alpha\beta\gamma}_{0j,R'j',R''j''}$, and the components of phonon eigenvectors, $\mathbf{e}_\lambda(l)$ with $l = j, j', \text{and } j''$ being the atomic index in unit cell. Here, α, β, and γ stand for the Cartesian components.

Phonons can be scattered by the boundaries of a finite size crystal. Phonon-boundary scattering is important, especially at low temperature and in nanostructures. $\tau_\lambda^{\mathrm{B}}$ the relaxation time of the phonon-boundary scattering can be obtained as [47–49]:

$$\frac{1}{\tau_\lambda^{\mathrm{B}}} = \frac{|v_\lambda|}{L}\frac{1-P}{1+P}, \tag{9}$$

where L is the length of the system and P is specularity parameter which ranges from zero for a diffusive scattering to unity for a specular scattering process. Therefore, $\tau_\lambda^{\mathrm{B}}$ includes the finite size effect in the thermal conductivity calculations.

Another source of scattering is associated with the silicon isotopes. Silicon has several isotopes among which, ^{28}Si is the most abundant (92.2%) and ^{29}Si (4.7%) and ^{30}Si (3.1%) are stable too [23]. One needs to account for the isotope scattering in order to calculate the thermal conductivity of naturally occurring silicene (silicene structure with natural composition of silicon isotopes). The phonon-isotope scattering due to mass-difference of isotopes can be expressed as [35, 45, 50, 51]:

$$\frac{1}{\tau_\lambda^{\mathrm{Iso}}} = \frac{\pi}{2N_0}\omega_\lambda^2 \sum_l g_l \sum_{\lambda'} |\mathbf{e}^*_\lambda(l).\mathbf{e}_{\lambda'}(l)|^2 \times \delta(\omega_\lambda - \omega_{\lambda'}), \tag{10}$$

where g_l is the mass variance parameter of the lth atom and defined as: [35, 50, 51]

$$g_l = \sum_i f_{il}(1 - \frac{M_{il}}{\bar{M}_l})^2, \tag{11}$$

with f_{il} being the concentration of ith isotope, M_{il} is the mass of ith isotope and $\bar{M}_l$ is the average atomic mass of the lth atom. For silicene, because of its monatomic structure, we have $f_{il} = f_i$ and $M_{il} = M_i$.

From the other side, real crystals naturally possess vacancy defects which affect the lattice thermal conductivity, significantly. Using perturbation theory, Klemens studied the scattering of phonons from the static imperfections such as vacancy defects [52, 53]. Phonon-vacancy scattering is expressed in terms of the missing mass, missing linkages and change of the force constant between under coordinated atoms near the vacancy defects. The phonon relaxation time due to the missing mass and missing linkages can be determined from [52–54]

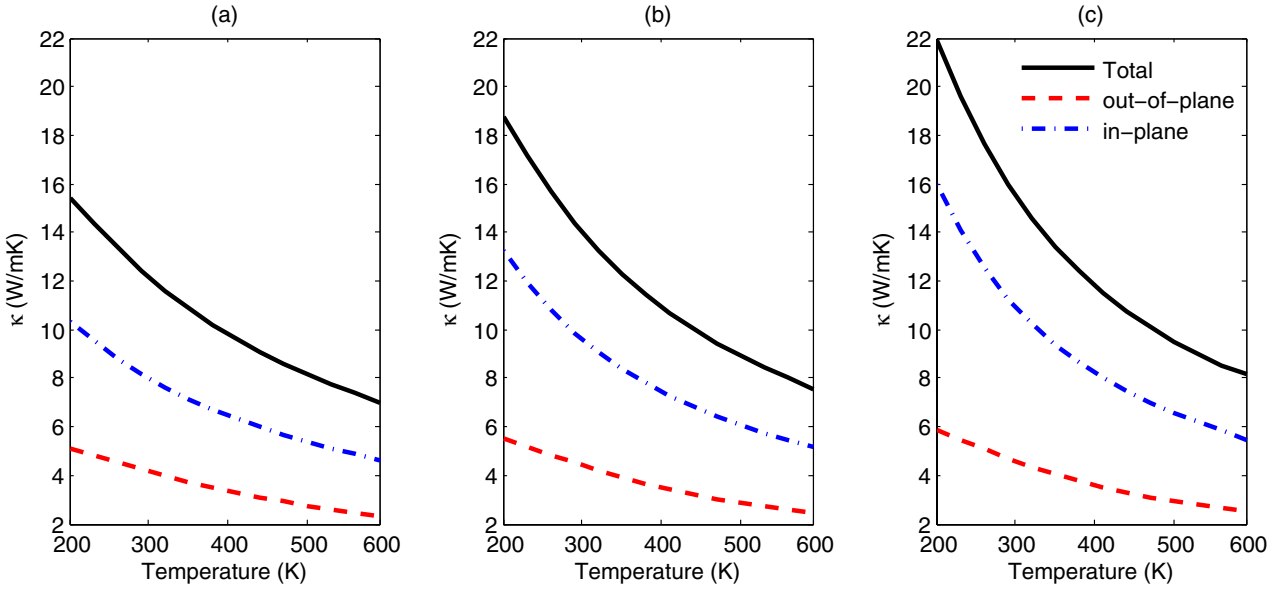

Figure 3. Temperature dependence of the intrinsic thermal conductivity of silicene for different lengths with the same specularity parameter, $P = 0$: (a) $L = 100$ nm, (b) $L = 300$ nm and (c) $L = 3$ μm.

$$\frac{1}{\tau_\lambda^{V_1}} = x\left(\frac{\triangle M}{M}\right)^2 \frac{\pi\omega_\lambda^2 g(\omega_\lambda)}{4N_0}, \tag{12}$$

where x, M and $g(\omega_\lambda)$ are the ratio of the vacancy defects concentration to the silicene atoms concentration, average mass of the atom and phonon density of states, respectively. Following [54], we set $\triangle M/M = -2 - (M_{\text{mis}}/M)$ where M_{mis} is the mass of the missing atom. Also, the force constant change contribution to the relaxation time is given by [54]

$$\frac{1}{\tau_\lambda^{V_2}} = x\left(\frac{\delta k}{k}\right)^2 \frac{2\pi\omega_\lambda^2 g(\omega_\lambda)}{N_0}, \tag{13}$$

with k being the average stiffness. The change in force constant of bonds between under-coordinated atoms in the bond-order-length-strength notation can be expressed as [54]

$$\left(\frac{\delta k}{k}\right) = \left[\frac{1+\exp[(12-z)/(8z)]}{1+\exp[(13-z)/(8z-8)]}\right]^{-m+2} - 1, \tag{14}$$

where z is the coordination number and m is a parameter that represents the nature of the bond. For Si the value of m has been optimized to be 4.88 [54–57].

3. Results and discussion

3.1. Intrinsic thermal conductivity

To investigate the thermal transport in silicene, we first calculate the intrinsic thermal conductivity of the free-standing clean (pure and defectless) silicene by considering the phonon–phonon scattering with $P = 0$ (a diffusive phonon-boundary scattering). Figure 3 displays temperature dependence of the thermal conductivities obtained from the in-plane, out-of-plane and total modes contributions to the intrinsic thermal conductivity for three different lengths, $L = 100$ nm, 300 nm and 3 μm. It should be pointed out that the thermal conductivity of silicene with $L = 3$ μm is obtained around 15.5 W mK^{-1}, while its value is about 150 W mK^{-1} for the bulk silicon at room temperature. Similar decrease in thermal conductivity of the silicon nanowires and thin films has been experimentally reported [23].

The presence of small buckling in silicene leads to a different contribution of phonon modes, compared to the planar structures [26, 27]; and as a result, an order of magnitude reduction in thermal conductivity is predicted [26]. Moreover, strong scattering of the flexural modes from the in-plane phonon modes yields a low value for the thermal conductivity of silicene [26]. We find that the in-plane acoustic modes are responsible for about 70% of total intrinsic thermal conductivity of silicene at room temperature and play a major role in increasing κ with the sample length (see figure 3), as it was pointed out earlier by Gu *et al* [27]. In addition, it can be seen that increasing the temperature leads to a reduction in κ which is expected for phonon-dominated systems in which the phonon–phonon scattering grows with temperature. Because of the buckled structure of silicene, the symmetry selection rule which applies to the case of graphene [58], does not apply here and therefore, the out-of-plane modes experience more scattering channels and as a result, their contribution to the thermal conductivity is smaller compared to the case of graphene [58].

3.2. Effect of phonon-boundary scattering

Figure 4 shows the change of κ with specularity parameter for three different sample sizes as a function of temperature. The thermal conductivity of pure and defectless silicene increases with growing the specularity parameter. When P value varies from zero to unity, the nature of the phonon-boundary scattering turns from completely diffusive to specular and as a result, the thermal conductivity increases and the influence of sample size on the phononic transport becomes weaker [17].

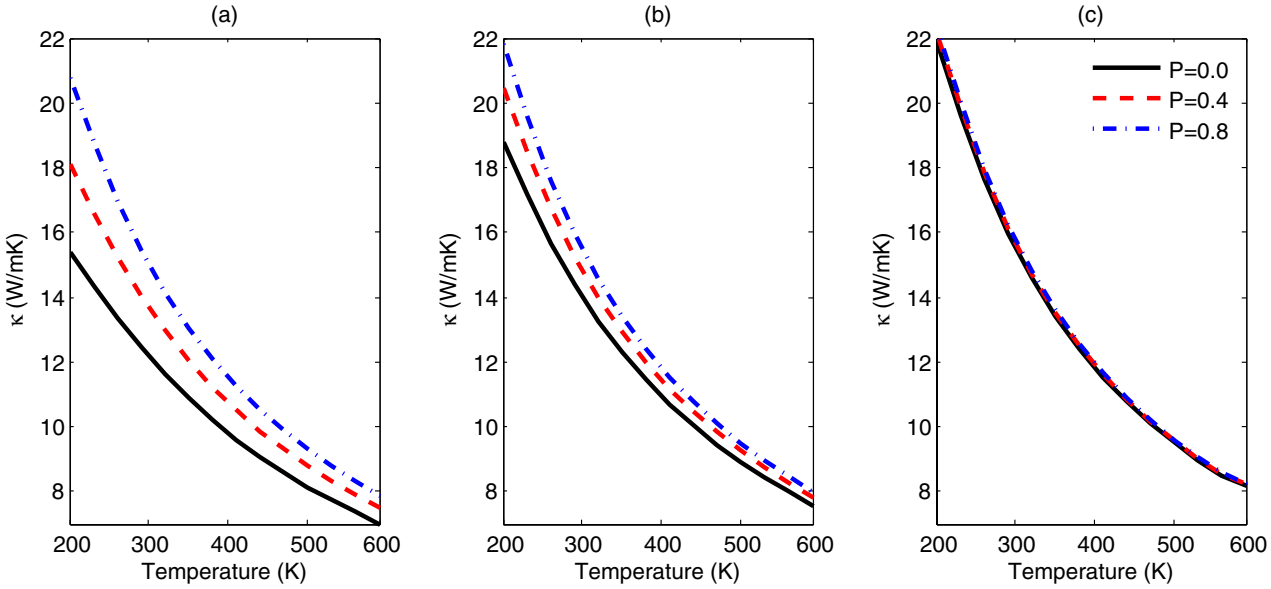

Figure 4. Temperature dependence of thermal conductivity of silicene for different specularity parameters, $P = 0, 0.4$ and 0.8 and different lengths:(a) $L = 100$ nm, (b) $L = 300$ nm and (c) $L = 3$ μm.

Also, the change of the thermal conductivity of small-size silicene by the specularity parameter is more pronounced at low temperatures. In fact, increasing temperature enhances the strength of phonon–phonon scattering which is the dominant scattering mechanism and therefore, phonon-boundary scattering effect gets reduced. It is worth pointing out that the effect of phonon-boundary scattering is negligible for samples with large size (see figure 4). Taking a look at equation (9), one learns that the relaxation time is proportional to the sample size which itself inversely contributes to the thermal conductivity, equations (1) and (3).

To complete this subsection, we should mention that because of a lower phonon group velocity in silicene, compared with graphene [8], the thermal conductivity of silicene is much less sensitive to the size effect (see equation (9)).

3.3. Effect of phonon-isotope scattering

The room-temperature thermal conductivity of naturally occurring silicene and pure silicene for two sample sizes are listed in table 1. As it is shown, the effect of isotopic scattering in silicene is much smaller than that in graphene [8, 58]. This discrepancy stems from the difference in the masses of Si and C atoms [8]. According to equations (10) and (11), the isotopic scattering rate depends upon $(1 - M_{il}/\bar{M}_l)^2$. A larger atomic mass of Si with respect to C, makes this ratio smaller, resulting in a weaker isotopic scattering effect on the thermal conductivity.

3.4. Effect of phonon-vacancy defect scattering

In this subsection, we study the effect of single vacancy defects on the thermal conductivity of free-standing silicene. Figure 5 shows the change of κ with the single vacancy defect concentration as a function of temperature for three different sample lengths when the phonon-boundary scattering is considered to be purely diffusive ($P = 0$).

Table 1. Thermal conductivity of pure and naturally occurring silicene at $T = 300$ K.

Size (μm)	$\kappa_{\mathbf{Pure}}$ (W mK^{-1})	$\kappa_{\mathbf{Natural}}$ (W mK^{-1})
0.3	14	13.7
3	15.5	15

The calculations presented in this figure suggest that the presence of a single vacancy defect significantly reduces the thermal conductivity values in silicene specially at low temperatures. By increasing temperature, the population of excited phonon modes increases and, as a result, the phonon–phonon scattering becomes dominant and makes the phonon-vacancy effect on the thermal conductivity weaker. Also, it can be observed that the thermal conductivity reduction due to the vacancy scattering is much stronger than the isotopic one (see table 1). A smaller coordination number in 2D materials compared to bulk materials, leads to a larger change in the force constants for those atoms which are close enough to the vacancy. Therefore, unlike the isotopic substitution effect, the phonon-vacancy defect scattering has a dominant impact on the thermal conductivity in silicene.

To get clearer insight, we focus on the influence of the single vacancy defects concentration at a fixed (room) temperature. Figure 6 depicts the changes of thermal conductivity of silicene versus single vacancy concentration for three different lengths at $T = 300$ K. According to this figure, while κ decreases remarkably with increasing vacancy percentage, the behavior of thermal conductivity as a function of vacancy concentration, for different sample sizes, is unchanged.

Our calculations show that even at the smallest single vacancy concentration studied here, 0.25%, i.e. the case in which only one of the every 400 atoms of Si is removed, the

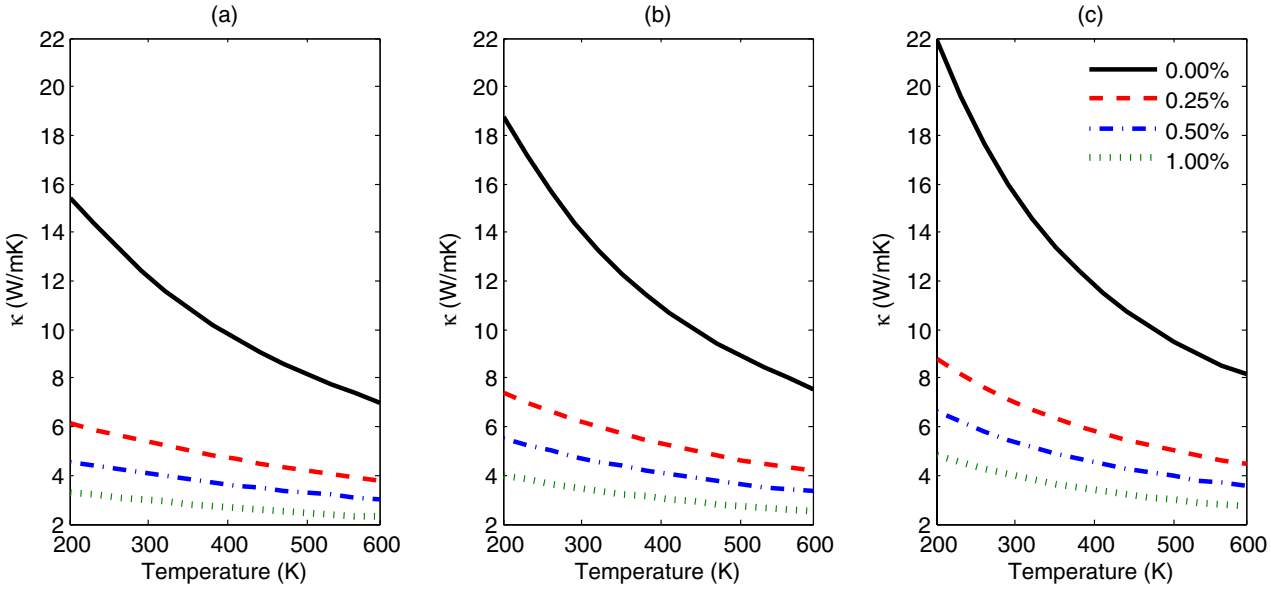

Figure 5. Effect of single vacancy defects on the thermal conductivity of free-standing silicene for different lengths with $P = 0$: (a) $L = 100$ nm, (b) $L = 300$ nm and (c) $L = 3$ μm.

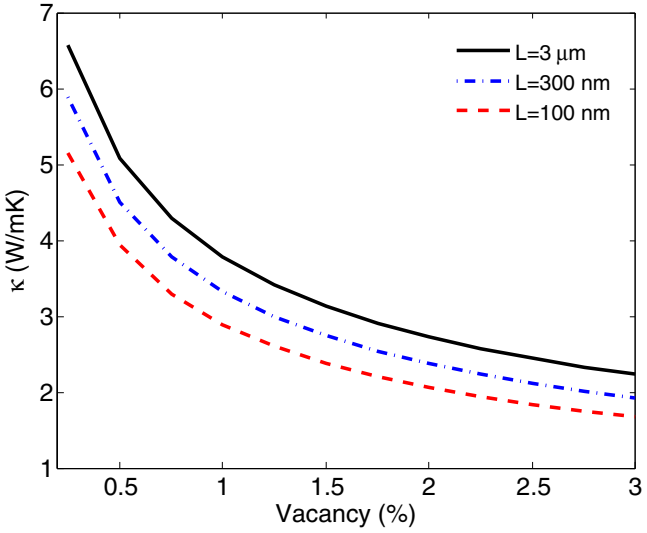

Figure 6. Thermal conductivity of free-standing silicene versus vacancy concentration for three different lengths with $P = 0$ at $T = 300$ K.

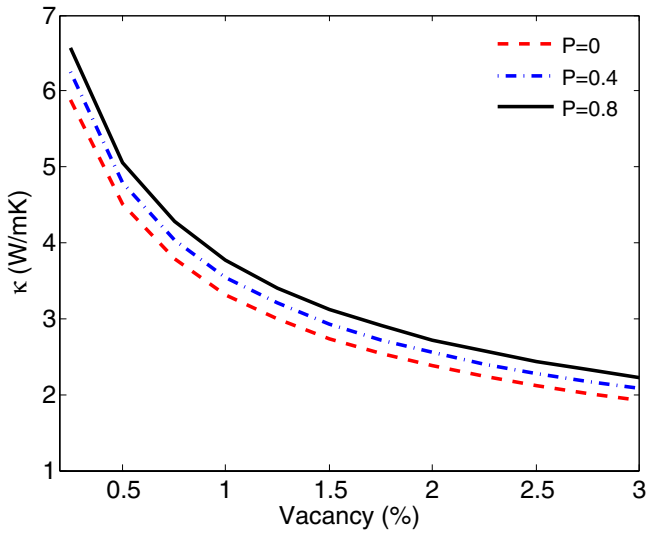

Figure 7. Thermal conductivity of free-standing silicene versus vacancy concentration for different specularity parameters with $L = 300$ nm at $T = 300$ K.

reduction in the thermal conductivity is substantial (≈58%). According to figure 6, our results predict that the significant reduction in the thermal conductivity of silicene happens for the concentrations less than 2% and beyond that it slows down, gradually. From equations (12) and (13) it is obvious that the relaxation times due to the missing mass and linkages and change in the force constant are inversely proportional to the concentration of single vacancy defects. Therefore, an enhancement in the single vacancy concentration leads to a reduction in the relaxation time as well as its contribution to the thermal conductivity.

Also, variation of the thermal conductivity in silicene as a function of single vacancy concentration for three different specularity parameters with $L = 3$ nm at room temperature is illustrated in figure 7. One can see the reduction of κ with increasing the vacancy percentage is not affected by the boundary scattering, similar to the result of figure 6. This indicates that the effect of single vacancy defects in comparison to the effects of sample length and specularity parameter is dominant in silicene.

In figure 8, the changes of lattice thermal conductivity with the vacancy defect percentage and temperature are shown, simultaneously. As we can see, the effect of vacancy defects on the thermal conductivity of silicene is stronger than that of temperature.

3.5. In-plane and out-of-plane phonons contributions to the thermal conductivity in presence of different scattering mechanisms

In order to achieve deeper understanding of the phononic transport in silicene, we obtain the separate contributions from the in-plane and out-of-plane phonon branches to the

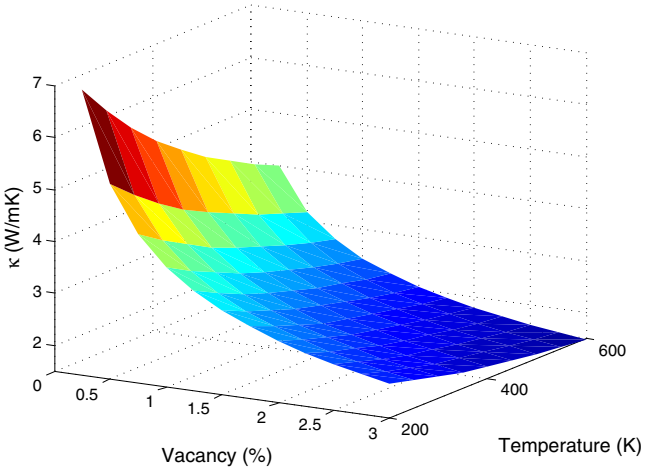

Figure 8. Thermal conductivity of free-standing silicene as a function of single vacancy defect concentration and temperature with $L = 100$ nm and $P = 0$.

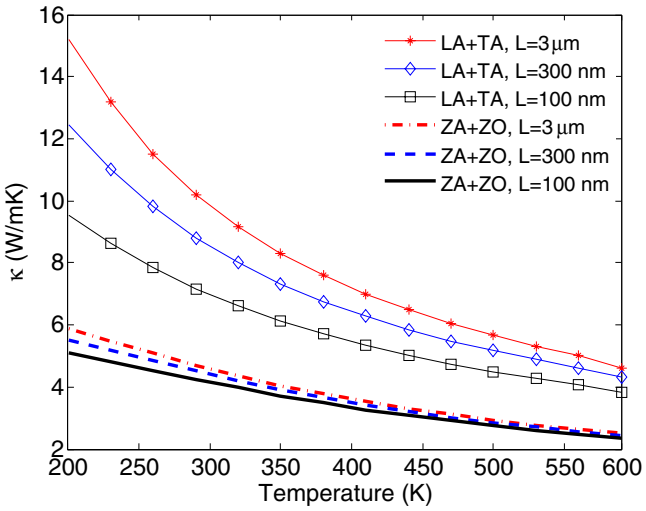

Figure 9. Contributions to the thermal conductivity from the in-plane and out-of-plane phonon modes as a function of temperature for three different sample sizes with $P = 0$.

thermal conductivity when another type of scattering mechanism exists. Figure 9 illustrates the results of calculations for three different lengths of clean silicene with $P = 0$. Because of small contributions of LO and TO modes at room temperature, these branches may be safely neglected. On the other hand, the dominant contribution to the thermal conductivity of silicene comes from the in-plane acoustic branches, which is about 70% of the thermal conductivity for $L = 3$ μm at $T = 300$ K. As temperature increases, the contribution of optical branches grows and, for instance at $T = 600$ K, the contribution of in-plane acoustic modes decreases to about 57%. As mentioned earlier, due to the buckled structure of silicene in comparison to the other planar 2D structures, the symmetry selection rule does not apply [26, 58, 59]. Therefore, the out-of-plane branches have more scattering channels than those in the planar structures. As a result, the contributions of the out-of-plane branches to the thermal conductivity are decreased. Moreover, increasing temperature strengthens the

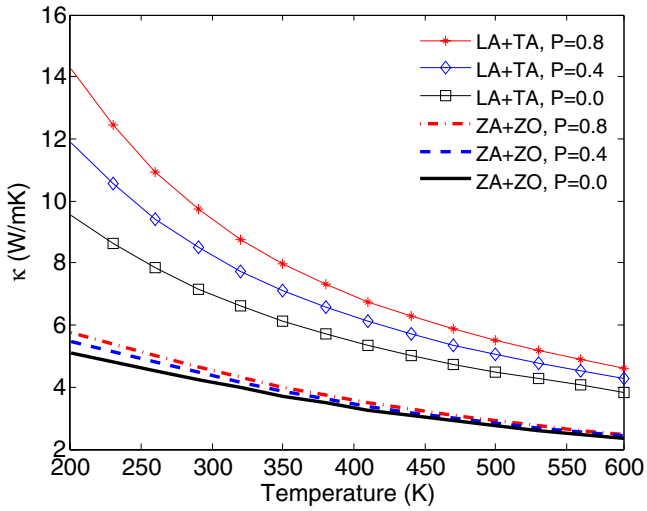

Figure 10. Contributions to the thermal conductivity from the in-plane and out-of-plane phonon modes as a function of temperature for different specularity parameters with $L = 100$ nm.

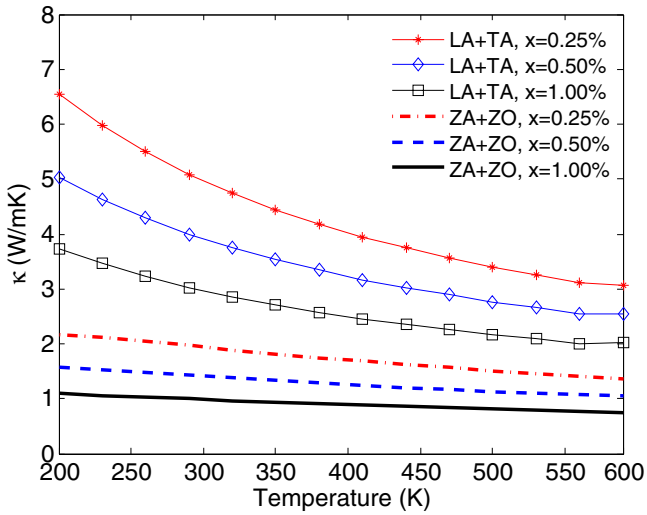

Figure 11. Thermal conductivity of the in-plane and out-of-plane branches as a function of temperature for different concentrations of single vacancy defects with $L = 3$ μm and $P = 0$.

phonon–phonon scattering and weakens other effects like sample size effect (see figure 9).

Also, the temperature dependence of the thermal conductivity associated to the in-plane and out-of-plane phonon branches of pure and defectless silicene with fixed sample size of 100 nm for different specularity parameters is shown in figure 10. As it is expected for 2D structures, the effect of phonon-boundary scattering on the contribution of the out-of-plane branches is very smaller than that in the case of in-plane branches. At high temperatures, again, it can be observed that the phonon–phonon scattering mechanism dominants and diminishes the influence of the phonon-boundary scattering.

Finally, figure 11 displays the contributions from the in-plane and out-of-plane modes to the thermal conductivity as a function of temperature for three different concentrations of single vacancy defects for a sample size of $L = 3$ μm with $P = 0$. Comparing this figure with figures 9 and 10, we find

that contrary to the previous cases, the contributions to the thermal conductivity from the out-of-plane phonon modes change considerably with the variation of vacancy defects concentration. However, the phononic transport due to these modes are less sensitive to the change of temperature. According to figure 11, one may find out that the contributions from all phonon branches are strongly affected by the phonon-vacancy scattering, even at high temperatures, which highlights the important role of the vacancies in silicene for heat transfer applications. Also, we find that in the presence of vacancy defects, the contribution of in-plane acoustic modes to the thermal conductivity becomes larger with respect to the intrinsic case.

4. Conclusions

In this paper, we have used the linearized PBTE within the RTA to calculate the lattice thermal conductivity of free-standing silicene under different scattering mechanisms including the phonon–phonon, phonon-boundary, phonon-isotope and phonon-vacancy defect. We have also studied the effects of sample size and different phonon modes on the phononic transport in silicene. We have employed the second- and third-order force constants, calculated with DFT, to obtain the phonon dispersion and phonon–phonon interactions, respectively. Our calculations have shown that the suppression of thermal conductivity by vacancies is quite remarkable so as even; removing only one of every 400 Si atoms leads to a substantial reduction in thermal conductivity. The present results have demonstrated that the impact of single vacancy defects on the heat transfer is much more pronounced at low temperatures. In addition, we have obtained that while the effect of isotopes on heat transfer is small, the role of phonon-boundary scattering is important in silicene samples with small size and no vacancies. Moreover, the contributions of the in-plane and out-of-plane branches to the thermal conductivity of silicene have been investigated. It has turned out that the contribution from the in-plane acoustic modes is dominant (about 70% at room temperature) and grows as the vacancy population increases. Finally, we have found that, although the out-of-plane modes contribution to the thermal conductivity changes slowly with the sample size and specularity parameter, it depends clearly on the vacancy concentration. This work may be compared with a few previously published studies. In [21] the equilibrium and nonequilibrium molecular dynamics approaches as well as a combined anharmonic lattice dynamics and Boltzmann method were employed to calculate the thermal conductivity of silicene at a fixed temperature by using the optimized Stillinger–Weber potentials. There, the phonon–phonon scattering was the only considered mechanism of scattering and the calculated thermal conductivity was reported to be less than 10 W mK^{-1} with nearly zero contribution from out-of-plane branches. In [26], the silicene thermal conductivity was predicted from the first-principles method considering only the phonon–phonon scattering and the similar results as [21] were obtained. The effect of phonon-vacancy defects scattering on the lattice thermal conductivity in silicene was investigated in [25] at room temperature by using the molecular dynamics simulation. Other scattering mechanisms as well as the in-plane and out-of-plane modes analysis were ignored. Inclusion of all scattering mechanisms and a detailed analysis on different modes contributions have enabled us to present a more complete picture of the thermal conductivity in silicene,which can become useful in nanoelectronic engineering and applications.

Acknowledgments

We would like to thank Dr Ronggui Yang for providing us the third-order force constants of silicene through http://spot.colorado.edu/∼yangr/NUTS/NUTS_Pub.html. It is also our pleasure to thank Dr Lucas Lindsay for sharing some data on graphene with us.

ORCID iDs

T Vazifehshenas https://orcid.org/0000-0002-0308-6714

References

[1] Geim A K and Novoselov K S 2007 *Nat. Mater.* **6** 183
[2] Novoselov K S, Jiang D, Schedin F, Booth T J, Khotkevich V V, Morozov S V and Geim A K 2005 *Proc. Natl Acad. Sci. USA* **102** 10451
[3] Novoselov K S, Geim A K, Morozov S V, Jiang D, Zhang Y, Dubonos S V, Grigorieva I V and Firsov A A 2004 *Science* **306** 666
[4] Schedin F, Geim A K, Morozov S V, Hill E W, Blake P, Katsnelson M I and Novoselov K S 2007 *Nat. Mater.* **6** 652
[5] Novoselov K S, Geim A K, Morozov S V, Jiang D, Katsnelson M I, Grigorieva I V, Dubonos S V and Firsov A A 2005 *Nature* **438** 197
[6] Drummond N D, Zolyomi V and Fal V 2012 *Phys. Rev.* B **85** 075423
[7] Ni Z, Liu Q, Tang K, Zheng J, Zhou J, Qin R, Gao Z, Yu D and Lu J 2012 *Nano Lett.* **12** 113
[8] Peng B, Zhang H, Shao H, Xu Y, Ni G, Zhang R and Zhu H 2016 *Phys. Rev.* B **94** 245420
[9] Yang K, Cahangirov S, Cantarero A, Rubio A and DAgosta R 2014 *Phys. Rev.* B **89** 125403
[10] Houssa M, Dimoulas A and Molle A 2015 *J. Phys.: Condens. Matter* **27** 253002
[11] Cahangirov S, Topsakal M, Akturk E, Sahin H and Ciraci S 2009 *Phys. Rev. Lett.* **102** 236804
[12] Liu C C, Feng W and Yao Y 2011 *Phys. Rev. Lett.* **107** 076802
[13] Guzman-Verri G G and Yan Voon L C L 2007 *Phys. Rev.* B **76** 075131
[14] Xie H, Ouyang T, Germaneau E, Qin G, Hu M and Bao H 2016 *Phys. Rev.* B **93** 075404
[15] Balandin A A 2011 *Nat. Mater.* **10** 569
[16] Pop E, Varshney V and Roy A K 2012 *MRS Bull.* **37** 1273
[17] Nika D L and Balandin A A 2012 *J. Phys.: Condens. Matter* **24** 233203
[18] Xu X, Chen J and Li B 2016 *J. Phys.: Condens. Matter* **28** 483001
[19] Yan Z, Nika D L and Balandin A A 2015 *IET Circuits Devices Syst.* **9** 4–12
[20] Balandin A A 2015 *ECS Trans.* **67** 167

[21] Zhang X, Xie H, Hu M, Bao H, Yue S, Qin G and Su G 2014 *Phys. Rev.* B **89** 054310
[22] Hu M, Zhang X and Poulikakos D 2013 *Phys. Rev.* B **87** 195417
[23] Pei Q X, Zhang Y W, Sha Z D and Shenoy V B 2013 *J. Appl. Phys.* **114** 033526
[24] Ng T Y, Yeo J and Liu Z 2013 *Int. J. Mech. Mater. Des.* **9** 105
[25] Li H P and Zhang R Q 2012 *Europhys. Lett.* **99** 36001
[26] Xie H, Hu M and Bao H 2014 *Appl. Phys. Lett.* **104** 131906
[27] Gu X and Yang R 2015 *J. Appl. Phys.* **117** 025102
[28] Kuang Y D, Lindsay L, Shi S Q and Zheng G P 2016 *Nanoscale* **8** 3760
[29] Ward A, Broido D, Stewart D A and Deinzer G 2009 *Phys. Rev.* B **80** 125203
[30] Esfarjani K, Chen G and Stokes H T 2011 *Phys. Rev.* B **84** 085204
[31] Luo T, Garg J, Shiomi J, Esfarjani K and Chen G 2013 *Europhys. Lett.* **101** 16001
[32] Garg J, Bonini N, Kozinsky B and Marzari N 2011 *Phys. Rev. Lett.* **106** 045901
[33] Tian Z, Garg J, Esfarjani K, Shiga T, Shiomi J and Chen G 2012 *Phys. Rev.* B **85** 184303
[34] Shiomi J, Esfarjani K and Chen G 2011 *Phys. Rev.* B **84** 104302
[35] Li W, Lindsay L, Broido D A, Stewart D A and Mingo N 2012 *Phys. Rev.* B **86** 174307
[36] Garg J, Bonini N and Marzari N 2011 *Nano Lett.* **11** 5135
[37] Garg J and Chen G 2013 *Phys. Rev.* B **87** 140302
[38] Peierls R 1929 *Ann. Phys.* **395** 1055
[39] Srivastava G P 1990 *The Physics of Phonons* (Bristol: Adam Hilger)
[40] Li W, Carrete J, Katcho N A and Mingo N 2014 *Comput. Phys. Commun.* **185** 1747
[41] Spencer M and Morishita T 2016 *Silicene: Structure, Properties and Applications* (Berlin: Springer)
[42] Paulatto L, Mauri F and Lazzeri M 2013 *Phys. Rev.* B **87** 214303
[43] lindsay L, Broido D A and Mingo N 2009 *Phys. Rev.* B **80** 125407
[44] Holland M G 1964 *Phys. Rev.* **134** A471
[45] Broido D A, Ward A and Mingo N 2005 *Phys. Rev.* B **72** 014308
[46] Lindsay L and Broido D A 2012 *Phys. Rev.* B **85** 035436
[47] Li W, Carrete J and Mingo N 2013 *Appl. Phys. Lett.* **103** 253103
[48] Ziman J M 1960 *Electrons and Phonons* (London: Clarendon)
[49] Nika D L, Pokatilov E P, Askerov A S and Balandin A A 2009 *Phys. Rev.* B **79** 155413
[50] Lindsay L, Broido D A and Reinecke T L 2012 *Phys. Rev. Lett.* **109** 095901
[51] Tamura S I 1983 *Phys. Rev.* B **27** 858
[52] Ratsifaritana C A and Klemens P G 2005 *Int. J. Thermophys.* **8** 737
[53] Klemens P G and Pedraza D F 1994 *Carbon* **32** 735
[54] Xie G, Shen Y, Wei X, Yang L, Xiao H, Zhong J and Zhang G 2014 *Sci. Rep.* **4** 5085
[55] Sun C Q, Pan L K, Fu Y Q, Tay B K and Li S 2003 *J. Phys. Chem.* B **107** 5113
[56] Sun C Q, Li C M, Bai H L and Jiang E Y 2005 *Nanotechnology* **16** 1290
[57] Sun C Q 2007 *Prog. Solid State Chem.* **35** 1–59
[58] lindsay L, Broido D A and Mingo N 2010 *Phys. Rev.* B **82** 115427
[59] Lindsay L, Li W, Carrete J, Mingo N, Broido D A and Reinecke T L 2014 *Phys. Rev.* B **89** 155426